
GRAPH RETENTION NETWORKS FOR DYNAMIC GRAPHS

Qian Chang

School of Information Management
Central China Normal University
changqian@mails.ccnu.edu.cn

Xia Li

School of Information Management
Central China Normal University
lixia@ccnu.edu.cn

Xiufeng Cheng

School of Information Management
Central China Normal University
xiufengcheng@ccnu.edu.cn

ABSTRACT

In this work, we propose **Graph Retention Network** (GRN) as a unified architecture for deep learning on dynamic graphs. The GRN extends the core computational manner of retention to dynamic graph data as graph retention, which empowers the model with three key computational paradigms that enable training parallelism, $O(1)$ low-cost inference, and long-term batch training. This architecture achieves an optimal balance of effectiveness, efficiency, and scalability. Extensive experiments conducted on benchmark datasets present the superior performance of the GRN in both edge-level prediction and node-level classification tasks. Our architecture achieves cutting-edge results while maintaining lower training latency, reduced GPU memory consumption, and up to an 86.7x improvement in inference throughput compared to baseline models. The GRNs have demonstrated strong potential to become a widely adopted architecture for dynamic graph learning tasks. Code will be available at <https://github.com/Chandler-Q/GraphRetentionNet>.

1 Introduction

Dynamic graphs offer a flexible and powerful geometric framework for modeling complex real-world systems that evolve over time, such as ecosystems [1, 2], social networks [3, 4, 5], and traffic systems [6, 7, 8]. These structures capture the temporal dynamics of interactions between entities, allowing for a more nuanced understanding of processes that unfold in both spatial and temporal dimensions [9, 8]. The increasing relevance of dynamic graphs has propelled substantial interest in the development of dynamic graph learning methods [10, 11, 12], motivated by their broad applicability across domains.

As these systems become more prominent, the ability to model temporal dependencies and evolving relationships within them has become a central focus of research, leading to numerous advances in graph-based machine learning [13, 14, 15, 16, 17, 18]. However, several challenges continue to hinder the effectiveness, efficiency, and scalability of existing approaches. First, a critical challenge in the field lies in the inability to reconcile training parallelism with low-cost inference [19, 20, 21, 22], particularly in the context of dense, large-scale, and long-term dynamic graphs. As part of Temporal Graph Neural Network (TGNN) training, the data extraction process includes both retrieving feature data and aggregating information from the past, which can make training much less efficient [23]. On the other hand, the data volume related to dynamic graphs, which evolve continuously over time, is substantially larger than that of static graphs. TGNN models also require the storage of both long-term and short-term memory information to capture the evolving nature of graph data. This requirement leads to significant storage demands and computational overhead [24], particularly for real-time inference, where timely access to historical and current state information is essential.

Second, the issue of long-term dependencies presents another obstacle. Although some recent architectures have demonstrated the ability to retain information over relatively extended periods [14, 25, 26, 27], current models frequently struggle to efficiently leverage information from distant past interactions due to the limitations imposed by truncation and sampling strategies [22]. This capability is crucial for many real-world applications where long-term dependencies play a significant role.

Finally, most existing models rely on separate modules, such as recent sampling strategies [27, 28] and memory modules [29, 30, 31] to aggregate information, both of which often introduce trade-offs between computational efficiency and predictive accuracy. Sampling techniques, while reducing complexity, may overlook essential information, while

memory-based approaches can impose scalability constraints. This lack of a unified graph operator ultimately impacts the scalability of these models across diverse dynamic graph scenarios, limiting their broader applicability.

In this work, we aim to address the above limitations with a unified architecture.

Contributions. In this paper, we first propose Graph Retention Network (GRN) as a new unified deep learning architecture for dynamic graphs. The GRN can handle a wide range of tasks and data structures because of its flexible architecture. Second, the GRN has graph retention as its core computational mechanism which has three computational paradigms: the parallel paradigm allows for training parallelism, the recurrent paradigm allows for low-cost inference, and the chunk-wise paradigm, which combines the first two paradigms, allows for long-term batch training. Finally, GRN demonstrates state-of-the-art performance across a wide range of benchmark datasets. In addition to its superior performance, the GRN also exhibits lower training latency, reduced GPU memory cost, and higher throughput, making them a highly efficient solution for dynamic graph learning tasks.

2 Related Work

Early methods for learning on dynamic graphs typically utilized separate modules, with graph neural networks capturing structural information and recurrent neural networks handling temporal dependencies [26, 29, 32, 33, 15]. While intuitive, this modular approach faces challenges in scalability [34, 35, 36], particularly when applied to large, densely connected graphs with extensive temporal information. The necessity of maintaining both structural and temporal embeddings increases computational complexity [37, 38], which can severely impact training efficiency.

Efforts to enhance scalability in TGNNs often involve neighbor truncation [14, 39] and selective sampling [13, 15, 40, 41], allowing models to focus computational resources on the most relevant temporal interactions. These techniques are particularly beneficial for real-time reasoning, where rapid inference is critical and the ability to model both short-term and long-term dependencies is essential.

Recent approaches in TGNNs have introduced strategies to improve the efficiency of training over large-scale dynamic graphs. Advanced data batching techniques and optimized memory management pipelines have been developed to reduce data access costs [20], minimize redundant data handling [40], and use GPUs fully [14, 42]. Such methods reorganize training batches and streamline data transfers, significantly boosting throughput and lowering the computational burden. As a result, these techniques make it feasible to handle high-dimensional, large-scale datasets while maintaining model effectiveness.

Unified architectures have also gained traction as a way to integrate structural and temporal information within a single framework. These end-to-end models leverage unified graph operators [22, 43], truncation strategies [14], and flexible temporal encoding functions [25, 44] to maintain context over time, which reduces the need for complex post-training memory updates. By applying attention-based methods and causal masking to selectively aggregate information, these architectures effectively capture long-term dependencies in dynamic graph data while avoiding computational inefficiencies.

3 Background

3.1 Static Graphs

A static graph $\mathcal{G} = (\mathcal{V}, \mathcal{E})$ is a non-linear data structure composed of a set of nodes (also referred to as vertices) $\mathcal{V} = \{v_1, v_2, \dots, v_{|\mathcal{V}|}\}$ and edges $\mathcal{E} = \{(v_i, v_j) \mid i, j \in \{1, 2, \dots, |\mathcal{V}|\}\}$, where each edge (v_i, v_j) represents a connection between nodes v_i and v_j . Both nodes and edges can be associated with features, denoted by $X = \{x_1, x_2, \dots, x_{|\mathcal{V}|}\}$ and $E = \{e_{ij}\}^{|\mathcal{E}|}$, that encode information relevant to entities and structure within the graph. The edges in the graph can also be represented as an adjacency matrix $\mathbf{A} \in \mathbb{R}^{|\mathcal{V}| \times |\mathcal{V}|}$, where each entry A_{ij} indicates the presence or absence of an edge between nodes v_i and v_j , i.e.

$$A_{ij} = \begin{cases} 1 & \text{if } (v_i, v_j) \in \mathcal{E}, \\ 0 & \text{otherwise.} \end{cases}$$

In cases where the graph is directed, the adjacency matrix \mathbf{A} is asymmetric, meaning $A_{ij} \neq A_{ji}$ in general. For undirected graphs, the adjacency matrix is symmetric, i.e., $A_{ij} = A_{ji}$. Additionally, if the edges are weighted, the entries of \mathbf{A} can represent the corresponding edge weights, with $A_{ij} = w_{ij}$ where w_{ij} is the weight of the edge connecting nodes v_i and v_j . In the absence of a connection, the corresponding entry remains zero.

3.2 Dynamic Graphs

In dynamic graphs, temporal attributes are introduced to capture changes in both the node and edge structure over time. These graphs evolve continuously or discretely as nodes and edges can appear, disappear, or update their properties over time. Dynamic graphs are generally categorized into two main types due to the inherent properties of time.

Discrete-time Dynamic Graphs Discrete-time dynamic graphs (DTDGs) evolve in distinct, time-ordered snapshots $\{\mathcal{G}_1, \mathcal{G}_2, \dots, \mathcal{G}_T\}$ where each graph $\mathcal{G}_t = (\mathcal{V}_t, \mathcal{E}_t)$ represents the state of the graph at a specific time step t . Temporal updates occur at discrete intervals, and each snapshot captures the state of the nodes and edges at a given time. This formulation is well-suited for applications where data is collected or processed at regular intervals.

Continuous-time Dynamic Graphs In contrast, continuous-time dynamic graphs (CTDGs) allow for changes to occur continuously over time, where nodes and edges evolve irregularly and events are associated with specific timestamps. The graph is represented as a function of continuous time, $\mathcal{G}(t) = (\mathcal{V}(t), \mathcal{E}(t))$, where t is the timestamp. In this setting, nodes and edges can be updated or interacted at any point in time, making CTDGs particularly useful for modeling asynchronous events.

In this paper, we focus on the DTDGs and CTDGs because dynamic graphs can represent real-world system evolution and are motivating extensive research, though our architecture can also be used for static graphs.

3.3 Temporal Graph Neural Networks

A typical Temporal Graph Neural Network (TGNN) learns representations through a dynamic message-passing paradigm that aggregates information from the neighborhood of each node over time.

$$\underbrace{v_i^{(k)}}_{\text{update}} \leftarrow \gamma \left(v_i^{(k-1)}, \underbrace{\bigoplus_{j \in \mathcal{N}(i)} \phi \left(v_i^{(k-1)}, v_j^{(k-1)}, e_{ij}, t \right)}_{\text{aggregate}} \right) \quad (1)$$

where $\phi(\cdot)$ is the **message function** that generates messages between nodes v_i and v_j using their features, edge features e_{ij} at time t , \oplus denotes the **aggregation function** that combines messages from all neighboring nodes $j \in \mathcal{N}(i)$, and $\gamma(\cdot)$ is the **update function** that incorporates the aggregated messages and previous state of the node to update the node representation over time. This process creates node embeddings, which are subsequently utilized for various downstream tasks.

In this paper, we evaluate the effectiveness, efficiency, and scalability of representation learning through two typical tasks in dynamic graph learning: (i) **edge-level prediction**, which predicts whether v_i and v_j are connected at the time t ; (ii) **node-level classification**, which infers the state of v_i at t .

4 Graph Retention Networks

Graph retention networks (GRNs) comprise a stack of multiple GRN blocks, each of which integrates a Multi-head Graph Retention module. Within each block, the core computational operator is the graph retention mechanism, which is responsible for selectively retaining and propagating crucial graph information across temporal updates. This retention operator is complemented by a Feed-forward Network, which refines and transforms the retained graph representations to facilitate downstream tasks.

4.1 Graph Retention

Graph retention can be considered a dual form graph operator that aggregates information from source and destination nodes in a parallel or recurrent manner. As shown in Figure 1, given a destination node v_i^t at time-step t with feature vector \mathbf{x}_t^i and its corresponding set of source nodes (i.e., historical 1-hop neighbors) $\{v_t^j\}_{t=1}^{|\mathcal{N}(i)|}$, the embeddings $\{\mathbf{x}_t^j\}_{t=1}^{|\mathcal{N}(i)|}$ of the source nodes, along with the associated edge attributes $\{e_t^j\}_{t=1}^{|\mathcal{N}(i)|}$ with temporal order are first packed into \mathbf{X}^j and \mathbf{E}^j , where d is the dimension of embeddings. We also pack the time intervals $\{\Delta t_i\}_{i=1}^{|\mathcal{N}(i)|}$ between the time each interaction occurs and the current time as $\Delta \mathbf{T}$.

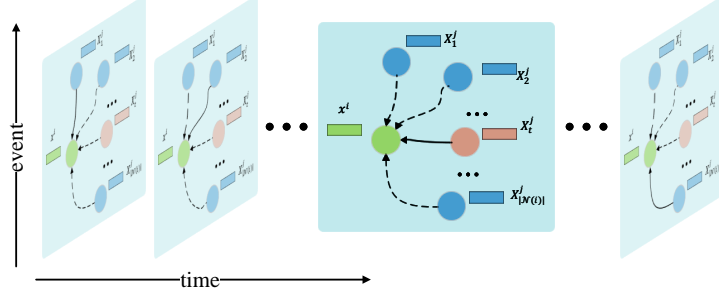


Figure 1: Continuous-time dynamic subgraph presentation.

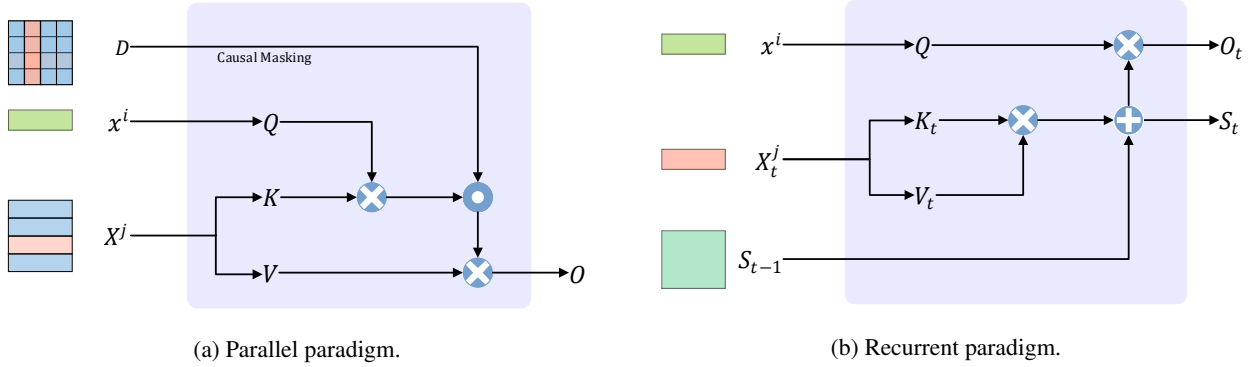


Figure 2: Dual form of GRN.

Here, we first use the message function to map the destination node features, edge attributes, and time intervals to the new feature space in a simple linear transformation, still denoted as \mathbf{X}^j .

$$\mathbf{X}^j = \text{msg}(\mathbf{X}^j, \mathbf{E}^j, \Delta\mathbf{T}) = \mathbf{X}^j + \mathbf{E}^j \mathbf{W}_e + \text{TE}(\Delta\mathbf{T}) \quad (2)$$

where $\mathbf{W}_e^j \in \mathbb{R}^{d \times d}$ is learnable weight matrix, and $\text{TE}(\cdot)$ is temporal encoding function described in Section 4.2.

Next, we denote graph retention as an aggregation function $\text{agg}(\mathbf{x}_t^i, \mathbf{X}^j)$ that maps $\mathbf{x}_t^i \xrightarrow{\text{agg}} o_t^i$, where $\Delta\mathbf{T}$ is the time intervals between the current timestamp t and the previous interaction timestamps. We first project \mathbf{x}_i to the query vector and \mathbf{X}^j to the key-value pairs as:

$$\mathbf{q} = \mathbf{x}^i \mathbf{W}_q + \mathbf{b}_q, \quad \mathbf{K} = \mathbf{X}^j \mathbf{W}_k + \mathbf{b}_k, \quad \mathbf{V} = \mathbf{X}^j \mathbf{W}_v + \mathbf{b}_v \quad (3)$$

where $\mathbf{W}_q, \mathbf{W}_k, \mathbf{W}_v \in \mathbb{R}^{d \times d}$ are learnable weight parameters, and $\mathbf{b}_q, \mathbf{b}_k, \mathbf{b}_v \in \mathbb{R}^d$ are bias terms for the query, key, and value projections, respectively.

Following the idea of the retention mechanism computation [45], we maintains a recurrent state \mathbf{S}^i for source node v_t^i . Then, we compute the output of graph retention in a recurrent manner:

$$\begin{aligned} \mathbf{S}_t^i &= \mathbf{S}_{t-1}^i + \mathbf{K}_t^T \mathbf{V}_t, & \mathbf{K}_t &\in \mathbb{R}^{1 \times d}, \mathbf{V}_t \in \mathbb{R}^{1 \times d} \\ \mathbf{o}_t^i &= \mathbf{q}_t \mathbf{S}_t^i = \sum_{t=1}^{|\mathcal{N}(i)|} \mathbf{q}_t \mathbf{K}_t^T \mathbf{V}_t, & \mathbf{q}_t &\in \mathbb{R}^{1 \times d} \end{aligned} \quad (4)$$

where we aggregate the source node with destination node through state matrix \mathbf{S}_t^i . The formulation of graph retention is easily parallelizable within training instances. We reformulate Equation (3) and (4) as follows for different training and inference situations.

Parallel Paradigm of Graph Retention Differ from sequence modeling, node-wise modeling in dynamic graphs does not involve self-interactions within the neighboring node set. The parallel paradigm of graph retention can be formulated as follows:

$$\begin{aligned} \mathbf{q} &= \mathbf{x}^i \mathbf{W}_q + \mathbf{b}_q, \quad \mathbf{K} = \mathbf{X}^j \mathbf{W}_k + \mathbf{b}_k, \quad \mathbf{V} = \mathbf{X}^j \mathbf{W}_v + \mathbf{b}_v \\ D_{tk} &= \begin{cases} w_t, & t \geq k \\ 0, & t < k \end{cases} \\ \text{GraphRetention}(\mathbf{x}^i, \mathbf{X}^j) &= (\mathbf{q} \mathbf{K}^\top \odot D) \mathbf{V} \end{aligned} \quad (5)$$

where D is a weighted causal mask to ensure that future nodes within the neighboring node set remain invisible to the current node, preserving causal structure during computation. The Hadamard product of $\mathbf{q} \mathbf{K}^\top$ and D will follow the broadcast mechanism for computation.

Recurrent Paradigm of Graph Retention As shown in Figure 2b, the recurrent paradigm of graph retention allows the model to iteratively aggregate information over sequential time steps, making it well-suited for long-term inference within dynamic graphs. At each time step t , the model updates the recurrent state \mathbf{S} based on the current key-value interaction:

$$\begin{aligned} \mathbf{S}_t &= \mathbf{S}_{t-1} + w_t \mathbf{K}_t^\top \mathbf{V}_t, \\ \text{GraphRetention}(\mathbf{x}_t^i, \mathbf{X}^j) &= \mathbf{Q}_t \mathbf{S}_t, \quad t = 1, \dots, |\mathcal{N}(i)| \end{aligned} \quad (6)$$

This recurrent mechanism enables the GRNs to retain and low-cost update node embeddings across time, facilitating the learning of complex temporal dependencies.

Chunk-wise Paradigm of Graph Retention To enable efficient training on the long-term and dense CTDGs, we utilize a hybrid form of parallel and recurrent paradigms. This computational paradigm splits the CTDGs into multiple stages, treating each stage as a distinct training batch, thereby conserving memory by training the model in manageable chunks. We formulate the chunk-wise paradigm of graph retention at the m -th stage as follows:

$$\begin{aligned} \mathbf{q}_{[m]} &= \mathbf{x}_{m-1}^i \mathbf{W}_q + \mathbf{b}_q, \quad \mathbf{K}_{[m]} = \mathbf{X}_{B:B(m+1)}^j \mathbf{W}_k + \mathbf{b}_k, \quad \mathbf{V}_{[m]} = \mathbf{X}_{Bm:B(m+1)}^j \mathbf{W}_v + \mathbf{b}_v \\ D_{tk} &= \begin{cases} w_t, & t \geq k \\ 0, & t < k \end{cases} \\ \text{GraphRetention}(\mathbf{x}^i, \mathbf{X}^j) &= (\mathbf{q} \mathbf{K}^\top \odot D) \mathbf{V} \end{aligned} \quad (7)$$

where B is batch size, $\mathbf{W}_q, \mathbf{W}_k, \mathbf{W}_v$ are the identical as in Equation (3). The chunk-wise paradigm without causal masking is also applicable for DTDGs.

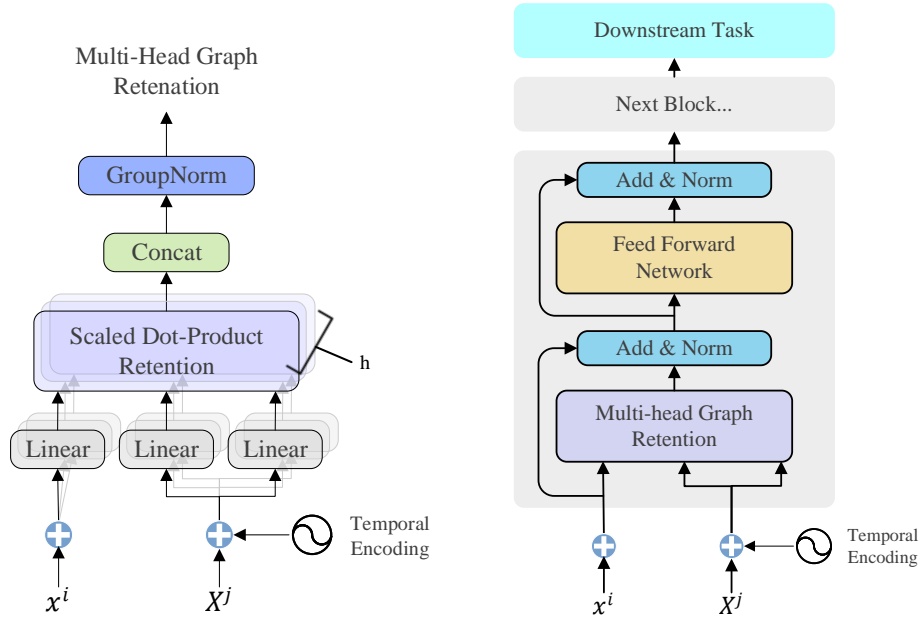
Finally, the output of graph retention serves as the representation for downstream tasks, and we update the destination node embedding for the subsequent iteration, i.e. $\mathbf{x}_{t+1}^i = o_t^i$.

4.2 Temporal Encoding

In this section, we introduce a temporal encoding mechanism from GraphMixer [44] into our architecture, which is designed to enable destination nodes to become time-aware of their neighboring nodes. Consider a specific time interval Δt , we define time-encoding function as:

$$\text{TE}(\Delta t, i) = \cos \left(\Delta t \cdot \sqrt{d}^{-(i-1)/\sqrt{d}} \right) \quad (8)$$

where i is the dimension of the encoding, and d denotes the overall dimension of the encoding space. The temporal encoding not only enriches the feature space but also aligns the model’s understanding with the intrinsic temporal nature of the underlying graph data.



(a) Architecture of the Multi-head Graph Retention.

(b) Architecture of GRNs.

4.3 Multi-head Graph Retention

Multi-head Graph Retention (MGR) extends the graph retention mechanism by enabling the model to simultaneously focus on information from multiple representation subspaces across different time intervals. This multi-head [46] approach captures complex temporal and relational dynamics for learning robust representations in dynamic graphs. We use h heads in the MGR layer as each head independently performs graph retention.

$$\begin{aligned} \text{head}_i &= \text{GraphRetention}(\mathbf{x}^i, \mathbf{X}^j) \\ \text{MGR}(\mathbf{x}^i, \mathbf{X}^j) &= \text{GN}(\text{Concat}(\text{head}_1, \text{head}_2, \dots, \text{head}_h)) \end{aligned} \quad (9)$$

where each head is associated with distinct projection parameters $\mathbf{W}_q, \mathbf{W}_k, \mathbf{W}_v \in \mathbb{R}^{d \times d}$, and group Normalization (GN) [47] is applied to the concatenated outputs of the heads to stabilize training and maintain numerical precision, ensuring consistency across heads despite varying information scales and distributions.

Graph Retention Score Normalization The GRN require normalization of the graph retention scores to maintain numerical stability within the computational process, i.e., 1) We normalize \mathbf{QK}^\top as $\mathbf{QK}^\top/\sqrt{d}$; 2) We replace \mathbf{D} with a scaled version $\tilde{\mathbf{D}}_{nm}$, where $\tilde{\mathbf{D}}_{nm} = \mathbf{D}_{nm}/\sum_{i=1}^n \mathbf{D}_{ni}$; 3) Let \mathbf{R} denote the retention scores, where $\mathbf{R} = \mathbf{QK}^\top \odot \mathbf{D}$, we further normalize \mathbf{R} as $\tilde{\mathbf{R}}_{nm} = \mathbf{R}_{nm}/\max(|\sum_{i=1}^n \mathbf{R}_{ni}|, 1)$. These operations will not influence the output of graph retention thanks to group normalization.

4.4 Overall Architecture of Graph Retention Networks

Each GRN block contains a MGR layer and a node-wise Feed-forward Network (FFN) module, forming the core components of the architecture. For an N -layer GRN, multiple GRN blocks are stacked to construct a deep learning network capable of capturing complex dependencies and structural nuances in dynamic graphs. The FFN module consists of two linear transformations with a h-swish [48] activation gate added between them to introduce nonlinearity.

For simplicity, we denote the inputs $\{\mathbf{x}^i, \mathbf{X}^j\}$ together as X and the embedding dimension of the FFN is defined as $d_{model} = h \times d$, where h is the number of heads and d is the dimension of each head. The general framework of GRN can be defined as:

$$\begin{aligned}
H &= \text{MGR}(\text{LN}(X)) + X \\
O &= \text{FFN}(\text{LN}(H)) + H
\end{aligned} \tag{10}$$

where $\text{FFN}(x) = (\text{hswish}(xW_1))W_2$

Where $\text{hswish}(x) = x \cdot \text{ReLU6}(x+3)/6 = x \cdot \min(\max(0, x+3), 6)/6$, $\text{LN}(\cdot)$ is layer normalization [49], and $W_1, W_2 \in \mathbb{R}^{d_{model} \times d_{model}}$ are learnable weight matrices in FFN for the integration of multiple retention outputs generated by the MGR.

5 Experiments

5.1 Setup

Datasets We conduct experiments on 14 benchmark datasets, which are from various domains and collected by [50]. Statistics of the datasets are shown in Table 1. We classify graphs as DTDGs when the number of links significantly exceeds the number of unique timesteps, as interactions within each batch primarily occur within a single temporal snapshot. More details for these datasets are illustrated in A.1.

Table 1: Statistics of datasets. Type: D = DTDG, C = CTDG; N.&F. Feat. = Node & Link Feature dimension.

Datasets	Type	Domains	Bipartite	#Nodes	#Links	#N.&L. Feat.	#Unique Steps	Duration	Time Granularity
Wikipedia	C	Social	True	9227	157474	- & 172	152757	1 month	Unix timestamps
Reddit	C	Social	True	10984	672447	- & 172	669065	1 month	Unix timestamps
MOOC	C	Interaction	True	7144	411749	- & 4	345600	17 months	Unix timestamps
LastFM	C	Interaction	True	1980	1293103	- & -	1283614	1 month	Unix timestamps
Myket	C	Interaction	True	17988	694121	- & -	693774	197 days	Unix timestamps
Enron	C	Social	False	184	125235	- & -	22632	3 years	Unix timestamps
Social Evo.	C	Proximity	False	74	2099519	- & 2	565932	8 months	Unix timestamps
UCI	C	Social	False	1899	59835	- & -	58911	196 days	Unix timestamps
Flights	D	Transport	False	13169	1927145	- & 1	122	4 months	days
Can. Parl.	D	Politics	False	734	74478	- & 1	14	14 years	years
US Legis.	D	Politics	False	225	60396	- & 1	12	12 congresses	congresses
UN Trade	D	Economics	False	255	507497	- & 1	32	32 years	years
UN Vote	D	Politics	False	201	1035742	- & 1	72	72 years	years
Contact	C	Proximity	False	692	2426279	- & 1	8064	1 month	5 minutes

Baselines We compare the GRN with nine strong baselines (JODIE[29], DyRep[41], TGAT[33], TGN[15], CAWN[28], EdgeBank[50], TCL[51], GraphMixer[44], and DyGFormer[14]), encompassing a variety of architectures, including GNNs, memory-based methods, transformers, and random walk approaches. These baseline models utilize truncation and sampling strategies to aggregate past information, while ours retains the recurrent state for graph retention. The delicate designs of these baselines represents most current ideas aimed at improving representation learning on dynamic graphs. Detailed descriptions of the baselines are given in A.2.

Downstream Tasks and Evaluation Metrics As illustrated in Section 3.3, we evaluate our model on edge-level prediction and node-level classification tasks. Specifically, we connect our model with a link predictor and a node classifier as downstream components. The components comprise multiple fully connected layers, with the link predictor estimating the connection probability between two nodes and the node classifier predicting the probability of a node belonging to a specific class. In addition, we evaluate the edge-level prediction task in both transductive and inductive settings. In dynamic graphs, transductive learning involves observing node and edge information during training, allowing the model to make predictions based on a known structure. In contrast, inductive learning requires the model to predict links between nodes that remain unobserved during training. We use Average Precision (AP) to assess model precision and the Area Under the Receiver Operating Characteristic Curve (AUC-ROC) to evaluate model sensitivity and robustness for both prediction and classification tasks. To measure training and inference efficiency, we compare models based on latency during training and inference, GPU memory consumption, and throughput.

Implementation and Configurations We follow the standard training and testing pipeline provided by the Dynamic Graph Library (DyGLib)¹ and Temporal Graph Benchmark (TGB)² to implement our model, adopting the DyGLib baseline scripts to ensure a consistent basis for comparison. For baselines requiring sampling, we utilize a random negative sampling strategy. The chunk-wise paradigm is applied for training, while inference adopts the recurrent

¹<https://github.com/yule-BUAA/DyGLib>

²<https://github.com/shenyangHuang/TGB>

computation paradigm to ensure that model retain identical long-term dependencies. The Adam optimizer with a binary cross-entropy loss function is used to optimize the training process, with a learning rate of 0.0001. Training is conducted over 50 epochs with an early stopping patience of 20 and a batch size of 200. Each model is trained and evaluated five times, with different random seeds assigned based on system time. For baseline models, we use the identical optimal configurations reported by DyGLib after validation, while the optimal configurations for our model are provided in Appendix A.3. All experiments are conducted on an Ubuntu operating system, utilizing an NVIDIA GeForce RTX 3090 GPU with 24GB of memory and an Intel Core i9-13900KF CPU.

5.2 Performance Comparison with Baselines

In this section, we present the results of our experiments, which are further detailed in the Appendix B.

Table 2: AP for transductive link prediction on dynamic graphs. The best and second-best performances are highlighted in bold and underlined fonts.

Datasets	JODIE	DyRep	TGAT	TGN	CAWN	EdgeBank	TCL	GraphMixer	DyGFormer	GRN
Wikipedia	89.30±1.11	83.18±0.92	92.80±0.56	92.58±0.33	98.07±0.04	90.37±0.00	93.92±0.17	94.48±0.07	<u>98.82±0.03</u>	100.0±0.00
Reddit	96.92±0.24	96.37±0.40	95.74±0.17	96.79±0.23	98.74±0.02	94.86±0.00	92.73±0.16	95.09±0.05	<u>98.96±0.06</u>	99.97±0.07
MOOC	61.11±1.66	62.11±1.65	<u>77.15±1.52</u>	74.33±2.48	66.56±1.20	57.97±0.00	74.36±1.45	72.87±0.46	70.34±1.10	100.0±0.00
LastFM	70.31±0.58	69.05±0.72	69.44±0.31	60.08±4.99	85.28±0.08	79.29±0.00	65.19±0.18	74.61±0.11	<u>91.59±0.02</u>	99.80±0.46
Myket	<u>86.88±0.06</u>	86.43±0.07	65.41±5.13	81.31±2.76	85.39±0.18	57.31±0.00	68.89±2.70	86.63±0.01	79.79±0.47	100.0±0.00
Enron	73.17±0.88	65.66±2.04	67.43±0.52	73.45±1.66	85.87±0.68	83.53±0.00	69.29±1.41	80.31±0.09	<u>87.17±2.13</u>	99.76±0.32
Social Evo.	75.82±2.21	78.91±3.66	91.19±0.32	89.84±0.64	84.18±0.06	74.95±0.00	91.52±0.18	90.93±0.19	<u>93.95±0.05</u>	99.77±0.18
UCI	87.96±0.68	53.19±2.19	77.51±0.67	86.52±0.98	93.08±0.13	76.20±0.00	84.17±0.80	91.90±0.70	<u>95.34±0.09</u>	99.81±0.31
Flights	90.73±1.35	87.64±0.97	90.79±0.02	92.18±1.31	96.83±0.24	89.35±0.00	89.36±0.17	89.43±0.01	<u>98.70±0.03</u>	99.56±0.96
Can. Parl.	69.22±0.38	63.40±1.73	67.69±1.18	68.53±0.85	67.25±3.15	64.55±0.00	65.51±2.56	75.42±0.52	<u>95.54±0.81</u>	99.97±0.07
US Legis.	<u>72.38±0.67</u>	61.79±1.79	61.45±2.50	69.69±0.36	65.88±1.23	58.39±0.00	60.89±0.67	70.08±0.66	70.36±0.38	98.34±3.68
UN Trade	61.37±0.37	58.82±0.73	60.27±0.78	60.23±0.57	<u>62.39±0.16</u>	60.41±0.00	60.64±0.31	54.12±4.50	57.03±1.42	97.26±4.69
UN Vote	56.83±0.79	57.46±0.28	51.71±0.41	55.55±1.01	51.58±0.05	<u>58.49±0.00</u>	51.59±0.14	51.71±0.11	53.26±0.13	99.96±0.08
Contact	89.00±3.18	79.03±2.55	93.45±0.17	91.79±1.99	87.23±0.21	92.58±0.00	89.01±0.54	89.31±0.30	<u>97.93±0.04</u>	99.60±0.30
Avg. Rank	5.57	8.00	6.21	5.79	5.07	7.36	7.00	5.50	3.50	1.00

Table 3: AUC-ROC for transductive link prediction on dynamic graphs.

Datasets	JODIE	DyRep	TGAT	TGN	CAWN	EdgeBank	TCL	GraphMixer	DyGFormer	GRN
Wikipedia	90.25±0.89	83.92±1.07	92.14±0.65	92.06±0.41	97.62±0.05	90.78±0.00	93.15±0.20	94.39±0.06	<u>98.65±0.04</u>	100.0±0.00
Reddit	96.87±0.21	96.37±0.41	95.73±0.14	96.79±0.23	98.54±0.03	95.37±0.00	92.71±0.15	94.97±0.04	<u>98.82±0.07</u>	99.98±0.05
MOOC	65.91±2.48	66.20±1.79	<u>78.22±2.04</u>	76.08±2.35	68.24±0.88	60.86±0.00	75.11±2.01	73.95±0.28	70.75±1.05	100.0±0.00
LastFM	70.02±0.57	68.58±0.91	68.79±0.28	57.81±3.99	83.52±0.15	83.77±0.00	62.87±0.18	73.30±0.04	<u>91.70±0.03</u>	99.79±0.47
Myket	<u>85.61±0.06</u>	85.03±0.07	66.00±5.63	80.28±3.36	83.72±0.16	57.35±0.00	68.87±2.18	85.08±0.03	78.94±0.39	100.0±0.00
Enron	79.40±0.70	69.72±1.95	65.55±0.71	74.43±2.27	85.56±0.92	87.05±0.00	67.46±1.39	83.66±0.10	<u>86.88±2.53</u>	99.75±0.34
Social Evo.	81.66±1.64	83.33±2.91	93.27±0.24	92.30±0.25	86.61±0.10	81.60±0.00	93.58±0.05	93.59±0.11	<u>95.77±0.05</u>	99.77±0.17
UCI	89.88±0.30	58.87±2.88	74.70±0.83	85.30±1.08	91.88±0.14	77.30±0.00	83.48±0.58	89.74±0.74	<u>93.87±0.13</u>	99.81±0.32
Flights	92.03±1.35	88.87±1.09	91.43±0.02	92.72±1.30	96.51±0.29	90.23±0.00	90.24±0.04	90.23±0.00	<u>98.71±0.04</u>	99.78±0.47
Can. Parl.	78.23±0.15	69.61±2.56	72.97±1.28	75.80±1.39	72.77±4.39	64.14±0.00	69.70±3.67	82.14±1.01	<u>96.23±0.93</u>	99.97±0.07
US Legis.	<u>81.08±0.40</u>	68.47±1.55	64.61±2.92	76.18±0.32	69.80±2.58	62.57±0.00	60.96±1.00	77.73±0.69	77.46±0.21	98.23±3.93
UN Trade	65.48±0.63	62.73±0.68	63.08±0.41	64.58±0.36	65.80±0.11	<u>66.75±0.00</u>	63.33±0.15	54.09±6.39	59.92±2.25	97.28±4.62
UN Vote	59.68±1.17	61.12±0.25	52.16±0.55	58.08±1.34	51.78±0.09	<u>62.97±0.00</u>	51.23±0.34	52.50±0.20	54.25±0.14	99.97±0.07
Contact	92.63±1.84	84.54±1.99	95.13±0.07	94.09±1.37	85.30±0.20	94.34±0.00	92.26±0.23	92.27±0.23	<u>98.17±0.04</u>	99.60±0.30
Avg. Rank	5.29	7.79	6.64	5.64	5.21	6.71	7.50	5.57	3.64	1.00

Our proposed GRN architecture consistently outperforms existing models across all experimental setups, demonstrating substantial improvements in both effectiveness and efficiency. Specifically, the GRNs achieve higher accuracy and more robust models, while simultaneously reducing latency, memory consumption, and improving throughput for both training and inference tasks. These results underscore the strong scalability of the GRNs and highlight the potential of a unified architecture for dynamic graph learning.

The experimental evaluation results are presented in Table 2,3, 6, and 7. In the edge-level prediction task, the GRNs exhibit near-perfect performance, with their AP outperforming baseline models across all datasets, in both transductive and inductive learning settings. Notably, on the US Legis., UN Trade, and UN Vote datasets, the GRNs achieve a remarkable improvement in AP, with a boost of up to 40%, representing a significant qualitative leap in performance. Furthermore, GRNs also secured the highest overall ranking in terms of AUC-ROC value. Nevertheless, as shown in Table 8, GRNs do not achieve optimal performance in the node classification task, particularly on the Reddit dataset. This underperformance is attributed to the extreme class imbalance present in the dataset, where the uneven distribution of categories hampers the model’s ability to learn effectively. This indicates that GRNs may struggle in scenarios with highly skewed class distributions, highlighting a potential area for future improvement.

We show the efficiency performance of training and inference in Figure 4. During training, the GRNs exhibit a latency reduction of 1.13x to 15.99x, a GPU memory consumption reduction of 1.53x to 3.55x, and a throughput improvement

of 1.17x to 16.61x compared to baseline models. The differences in inference efficiency are even more pronounced, with the GRNs demonstrating at least 6.1x lower latency, 1.66x less GPU usage, and an up to 86.7x improvement in throughput.

5.3 Ablation Study

Table 4: Evaluation performance of GRN variants. Unlisted values indicate that the dataset is not applicable in the certain variant.

Variants	AP			AUC		
	Eron	UCI	US Legis.	Eron	UCI	US Legis.
GRN	99.76±0.32	99.81±0.31	98.34±3.68	99.75±0.34	99.81±0.32	98.23±3.93
- w/o temporal encoding	98.75±2.31	99.64±0.42	-	96.29±2.02	99.67±0.46	-
- w/o h-swish gate	94.90±6.95	95.55±3.92	91.16±2.61	91.60±6.68	95.64±3.89	91.29±4.62
- w/o multi-head	70.58±8.13	84.87±2.41	89.35±1.31	69.83±5.87	84.56±2.50	89.92±2.18
- Reduce head dimension	87.09±1.57	95.73±0.42	96.10±1.51	86.40±1.72	95.84±0.41	96.30±1.65

To evaluate the contribution of individual components within the GRN architecture, we conduct a series of ablation experiments. Table 4 presents the performance of GRN variants, where specific architectural elements are systematically removed or altered.

The results highlight the importance of each component in achieving the superior performance of the full GRN model. The removal of temporal encoding results in a moderate performance drop, particularly evident in the AP scores for the Eron dataset. This underscores the critical role of temporal encoding in capturing temporal dependencies within dynamic graphs. The absence of the h-swish gate leads to a significant degradation in performance, with AP values dropping sharply across datasets (e.g., from 99.76±0.32 to 94.90±6.95 on Eron). This finding emphasizes the h-swish gate’s role in efficient non-linear transformations and its impact on model robustness.

The multi-head mechanism appears indispensable, as removing it (- w/o multi-head) results in the most pronounced decline in both AP and AUC metrics. For instance, the AP on Eron plummets, indicating that multi-head attention is essential for capturing diverse relational patterns in complex graph structures. Furthermore, reducing the head dimension (- Reduce head dimension) also negatively impacts performance, albeit to a lesser extent compared to other ablations. The slight decline in metrics, such as the AP on US Legis., suggests that a higher dimensionality in attention heads is beneficial for expressive power, though the model remains competitive under this constraint.

6 Conclusion

In this work, we introduce the GRN as a unified architecture that introduces the novel graph retention mechanism to address key challenges in dynamic graph learning. Through extensive experiments on the benchmark datasets, GRN demonstrates state-of-the-art performance, validating its robustness and versatility across diverse dynamic graph tasks. Our ablation studies further emphasized the importance of components. We have also stated our concerns and limitations in Appendix C, which we expect to address in the future.

References

- [1] Jie Li and Matteo Convertino. Inferring ecosystem networks as information flows. *Scientific reports*, 11(1):7094, 2021.
- [2] Mandani Ntekouli, Gerasimos Spanakis, Lourens Waldorp, and Anne Roefs. Exploiting individual graph structures to enhance ecological momentary assessment (ema) forecasting. In *2024 IEEE 40th International Conference on Data Engineering Workshops (ICDEW)*, pages 158–166. IEEE, 2024.
- [3] Shengjie Min, Zhan Gao, Jing Peng, Liang Wang, Ke Qin, and Bo Fang. Stgsn—a spatial–temporal graph neural network framework for time-evolving social networks. *Knowledge-Based Systems*, 214:106746, 2021.
- [4] Unai Alvarez-Rodriguez, Federico Battiston, Guilherme Ferraz de Arruda, Yamir Moreno, Matjaž Perc, and Vito Latora. Evolutionary dynamics of higher-order interactions in social networks. *Nature Human Behaviour*, 5(5):586–595, 2021.

- [5] Srijan Kumar, Xikun Zhang, and Jure Leskovec. Predicting dynamic embedding trajectory in temporal interaction networks. In *Proceedings of the 25th ACM SIGKDD international conference on knowledge discovery & data mining*, pages 1269–1278, 2019.
- [6] Bing Yu, Haoteng Yin, and Zhanxing Zhu. Spatio-temporal graph convolutional networks: A deep learning framework for traffic forecasting. *arXiv preprint arXiv:1709.04875*, 2017.
- [7] Zonghan Wu, Shirui Pan, Guodong Long, Jing Jiang, and Chengqi Zhang. Graph wavenet for deep spatial-temporal graph modeling. *arXiv preprint arXiv:1906.00121*, 2019.
- [8] Shengnan Guo, Youfang Lin, Huaiyu Wan, Xiucheng Li, and Gao Cong. Learning dynamics and heterogeneity of spatial-temporal graph data for traffic forecasting. *IEEE Transactions on Knowledge and Data Engineering*, 34(11):5415–5428, 2021.
- [9] Peter Battaglia, Razvan Pascanu, Matthew Lai, Danilo Jimenez Rezende, et al. Interaction networks for learning about objects, relations and physics. *Advances in neural information processing systems*, 29, 2016.
- [10] Yao Ma, Ziyi Guo, Zhaocun Ren, Jiliang Tang, and Dawei Yin. Streaming graph neural networks. In *Proceedings of the 43rd international ACM SIGIR conference on research and development in information retrieval*, pages 719–728, 2020.
- [11] Nan Yin, Mengzhu Wang, Zhenghan Chen, Giulia De Masi, Huan Xiong, and Bin Gu. Dynamic spiking graph neural networks. In *Proceedings of the AAAI Conference on Artificial Intelligence*, volume 38, pages 16495–16503, 2024.
- [12] Hanjie Li, Changsheng Li, Kaituo Feng, Ye Yuan, Guoren Wang, and Hongyuan Zha. Robust knowledge adaptation for dynamic graph neural networks. *IEEE Transactions on Knowledge and Data Engineering*, 2024.
- [13] Siwei Zhang, Xi Chen, Yun Xiong, Xixi Wu, Yao Zhang, Yongrui Fu, Yinglong Zhao, and Jiawei Zhang. Towards adaptive neighborhood for advancing temporal interaction graph modeling. In *Proceedings of the 30th ACM SIGKDD Conference on Knowledge Discovery and Data Mining*, pages 4290–4301, 2024.
- [14] Le Yu, Leilei Sun, Bowen Du, and Weifeng Lv. Towards better dynamic graph learning: New architecture and unified library. *Advances in Neural Information Processing Systems*, 36:67686–67700, 2023.
- [15] Emanuele Rossi, Ben Chamberlain, Fabrizio Frasca, Davide Eynard, Federico Monti, and Michael Bronstein. Temporal graph networks for deep learning on dynamic graphs. *arXiv preprint arXiv:2006.10637*, 2020.
- [16] John A Miller, Mohammed Aldosari, Farah Saeed, Nasid Habib Barna, Subas Rana, I Budak Arpinar, and Ninghao Liu. A survey of deep learning and foundation models for time series forecasting. *arXiv preprint arXiv:2401.13912*, 2024.
- [17] Jana Vatter, Ruben Mayer, and Hans-Arno Jacobsen. The evolution of distributed systems for graph neural networks and their origin in graph processing and deep learning: A survey. *ACM Computing Surveys*, 56(1):1–37, 2023.
- [18] Zeyang Zhang, Xin Wang, Ziwei Zhang, Haoyang Li, Yijian Qin, Simin Wu, and Wenwu Zhu. Llm4dyg: Can large language models solve problems on dynamic graphs? *arXiv preprint arXiv:2310.17110*, 2023.
- [19] Yuhong Luo and Pan Li. No need to look back: An efficient and scalable approach for temporal network representation learning. *arXiv preprint arXiv:2402.01964*, 2024.
- [20] Shihong Gao, Yiming Li, Yanyan Shen, Yingxia Shao, and Lei Chen. Etc: Efficient training of temporal graph neural networks over large-scale dynamic graphs. *Proceedings of the VLDB Endowment*, 17:1060–1072, 2024.
- [21] Yuxia Wu, Yuan Fang, and Lizi Liao. On the feasibility of simple transformer for dynamic graph modeling. In *Proceedings of the ACM on Web Conference 2024*, pages 870–880, 2024.
- [22] Hongkuan Zhou, Da Zheng, Israt Nisa, Vasileios Ioannidis, Xiang Song, and George Karypis. Tgl: A general framework for temporal gnn training on billion-scale graphs. *arXiv preprint arXiv:2203.14883*, 2022.
- [23] Hongkuan Zhou, Da Zheng, Xiang Song, George Karypis, and Viktor Prasanna. Distgl: Distributed memory-based temporal graph neural network training. In *Proceedings of the International Conference for High Performance Computing, Networking, Storage and Analysis*, pages 1–12, 2023.
- [24] ZhengZhao Feng, Rui Wang, TianXing Wang, Mingli Song, Sai Wu, and Shuibing He. A comprehensive survey of dynamic graph neural networks: Models, frameworks, benchmarks, experiments and challenges. *arXiv preprint arXiv:2405.00476*, 2024.
- [25] Shenyang Huang, Farimah Poursafaei, Jacob Danovitch, Matthias Fey, Weihua Hu, Emanuele Rossi, Jure Leskovec, Michael Bronstein, Guillaume Rabusseau, and Reihaneh Rabbany. Temporal graph benchmark for machine learning on temporal graphs. *Advances in Neural Information Processing Systems*, 36, 2024.

- [26] Aldo Pareja, Giacomo Domeniconi, Jie Chen, Tengfei Ma, Toyotaro Suzumura, Hiroki Kanezashi, Tim Kaler, Tao Schardl, and Charles Leiserson. Evolvegnn: Evolving graph convolutional networks for dynamic graphs. In *Proceedings of the AAAI conference on artificial intelligence*, volume 34, pages 5363–5370, 2020.
- [27] Da Xu, Chuanwei Ruan, Evren Korpeoglu, Sushant Kumar, and Kannan Achan. Inductive representation learning on temporal graphs. *arXiv preprint arXiv:2002.07962*, 2020.
- [28] Yanbang Wang, Yen-Yu Chang, Yunyu Liu, Jure Leskovec, and Pan Li. Inductive representation learning in temporal networks via causal anonymous walks. *arXiv preprint arXiv:2101.05974*, 2021.
- [29] Srijan Kumar, Xikun Zhang, and Jure Leskovec. Predicting dynamic embedding trajectory in temporal interaction networks. In *Proceedings of the 25th ACM SIGKDD international conference on knowledge discovery & data mining*, pages 1269–1278, 2019.
- [30] Jason Weston, Sumit Chopra, and Antoine Bordes. Memory networks. *arXiv preprint arXiv:1410.3916*, 2014.
- [31] Junwei Su, Difan Zou, and Chuan Wu. Pres: Toward scalable memory-based dynamic graph neural networks. *arXiv preprint arXiv:2402.04284*, 2024.
- [32] Franco Manessi, Alessandro Rozza, and Mario Manzo. Dynamic graph convolutional networks. *Pattern Recognition*, 97:107000, 2020.
- [33] Da Xu, Chuanwei Ruan, Evren Korpeoglu, Sushant Kumar, and Kannan Achan. Inductive representation learning on temporal graphs. *arXiv preprint arXiv:2002.07962*, 2020.
- [34] Stephen Bonner, Amir Atapour-Abarghouei, Philip T Jackson, John Brennan, Ibad Kureshi, Georgios Theodoropoulos, Andrew Stephen McGough, and Boguslaw Obara. Temporal neighbourhood aggregation: Predicting future links in temporal graphs via recurrent variational graph convolutions. In *2019 IEEE international conference on big data (Big Data)*, pages 5336–5345. IEEE, 2019.
- [35] Guangji Bai, Chen Ling, and Liang Zhao. Temporal domain generalization with drift-aware dynamic neural networks. *arXiv preprint arXiv:2205.10664*, 2022.
- [36] Jintang Li, Zhouxin Yu, Zulun Zhu, Liang Chen, Qi Yu, Zibin Zheng, Sheng Tian, Ruofan Wu, and Changhua Meng. Scaling up dynamic graph representation learning via spiking neural networks. In *Proceedings of the AAAI Conference on Artificial Intelligence*, volume 37, pages 8588–8596, 2023.
- [37] Peng Cui, Xiao Wang, Jian Pei, and Wenwu Zhu. A survey on network embedding. *IEEE transactions on knowledge and data engineering*, 31:833–852, 2018.
- [38] Dingyuan Zhu, Peng Cui, Ziwei Zhang, Jian Pei, and Wenwu Zhu. High-order proximity preserved embedding for dynamic networks. *IEEE Transactions on Knowledge and Data Engineering*, 30(11):2134–2144, 2018.
- [39] Franco Manessi, Alessandro Rozza, and Mario Manzo. Dynamic graph convolutional networks. *Pattern Recognition*, 97:107000, 2020.
- [40] Mingyu Guan, Anand Padmanabha Iyer, and Taesoo Kim. Dynagraph: dynamic graph neural networks at scale. In *Proceedings of the 5th ACM SIGMOD Joint International Workshop on Graph Data Management Experiences & Systems (GRADES) and Network Data Analytics (NDA)*, pages 1–10, 2022.
- [41] Rakshit Trivedi, Mehrdad Farajtabar, Prasenjeet Biswal, and Hongyuan Zha. Dyrep: Learning representations over dynamic graphs. In *International conference on learning representations*, 2019.
- [42] Xinchun Wan, Kaiqiang Xu, Xudong Liao, Yilun Jin, Kai Chen, and Xin Jin. Scalable and efficient full-graph gnn training for large graphs. *Proceedings of the ACM on Management of Data*, 1:1–23, 2023.
- [43] Yangjie Zhou, Jingwen Leng, Yaoxu Song, Shuwen Lu, Mian Wang, Chao Li, Minyi Guo, Wenting Shen, Yong Li, Wei Lin, et al. Ugrapher: High-performance graph operator computation via unified abstraction for graph neural networks. In *Proceedings of the 28th ACM International Conference on Architectural Support for Programming Languages and Operating Systems, Volume 2*, pages 878–891, 2023.
- [44] Weilin Cong, Si Zhang, Jian Kang, Baichuan Yuan, Hao Wu, Xin Zhou, Hanghang Tong, and Mehrdad Mahdavi. Do we really need complicated model architectures for temporal networks? *arXiv preprint arXiv:2302.11636*, 2023.
- [45] Yutao Sun, Li Dong, Shaohan Huang, Shuming Ma, Yuqing Xia, Jilong Xue, Jianyong Wang, and Furu Wei. Retentive network: A successor to transformer for large language models. *arXiv preprint arXiv:2307.08621*, 2023.
- [46] A Vaswani. Attention is all you need. *Advances in Neural Information Processing Systems*, 2017.
- [47] Yuxin Wu and Kaiming He. Group normalization. In *Proceedings of the European conference on computer vision (ECCV)*, pages 3–19, 2018.

- [48] Andrew Howard, Mark Sandler, Grace Chu, Liang-Chieh Chen, Bo Chen, Mingxing Tan, Weijun Wang, Yukun Zhu, Ruoming Pang, Vijay Vasudevan, et al. Searching for mobilenetv3. In *Proceedings of the IEEE/CVF international conference on computer vision*, pages 1314–1324, 2019.
- [49] Jimmy Lei Ba. Layer normalization. *arXiv preprint arXiv:1607.06450*, 2016.
- [50] Farimah Poursafaei, Shenyang Huang, Kellin Pelrine, and Reihaneh Rabbany. Towards better evaluation for dynamic link prediction. *Advances in Neural Information Processing Systems*, 35:32928–32941, 2022.
- [51] Lu Wang, Xiaofu Chang, Shuang Li, Yunfei Chu, Hui Li, Wei Zhang, Xiaofeng He, Le Song, Jingren Zhou, and Hongxia Yang. Tcl: Transformer-based dynamic graph modelling via contrastive learning. *arXiv preprint arXiv:2105.07944*, 2021.

A Detailed Experimental Settings

A.1 Descriptions of Datasets

We describe many details of the dataset³ below:

- **Wikipedia** comprises records of edits to Wikipedia pages over a 1-month period, representing a bipartite CTGD in the social networking domain. Nodes correspond to editors and Wikipedia pages, while edges represent editing behaviors annotated with timestamps. Each edge includes a 172-dimensional Linguistic Inquiry and Word Count (LIWC) feature. The dataset also contains dynamic labels indicating whether a user has been temporarily banned from editing.
- **Reddit** captures user posting behavior within Reddit sub-sections over a 1-month period and is a bipartite CTGD in the social networking domain. Nodes represent users and posts, while edges denote posting interactions with timestamps. Each edge includes a 172-dimensional LIWC feature, alongside dynamic labels indicating whether a user has been banned from posting.
- **MOOC** is a student interaction network from a 17-month span of online course content usage, this bipartite CTGD has nodes representing students and course content units (e.g., videos or question sets). Edges represent student behaviors in accessing specific content units, each annotated with 4 features.
- **LastFM** tracks user song-listening behaviors over a 1-month period, forming a CTGD. Nodes correspond to users and songs, and edges indicate listening interactions. No additional features are provided.
- **Myket** is derived from the Myket app marketplace, this bipartite CTGD records app download interactions among users over 197 days. Nodes represent users and apps, while edges denote download events. The dataset does not include additional features.
- **Myket** captures email communication behaviors among employees of ENRON Energy over a 3-year period, forming a CTGD in the social networking domain. Nodes represent employees, and edges correspond to email exchanges. No additional features are available.
- **Social Evo** is a cell phone contact network documenting the daily lives of university dormitory residents over an 8-month period. This CTGD captures proximity-based interactions, with edges containing 2 features.
- **UCI** represents online communication among approximately 1,900 students at the University of California, Irvine, and this CTGD spans 196 days. Nodes correspond to students, and edges capture message exchanges. No additional features are provided.
- **Flights** is a directed dynamic flight network describing the evolution of air traffic over 4 months during the COVID-19 pandemic. Nodes represent airports, and edges indicate tracked flights, with weights reflecting the number of flights between two airports on a given day.
- **Can. Parl.** is a weighted dynamic political network tracking interactions between Canadian Members of Parliament (MPs) from 2006 to 2019. Nodes represent MPs, while edges indicate co-voting behavior, with weights reflecting the number of times two MPs voted “yes” on the same bill.
- **US Legis.** represents a co-sponsorship graph capturing social interactions among U.S. Senators, with edge weights representing the number of times two senators co-sponsored a bill within the same Congress.
- **UN Trade** describes food and agricultural trade among 181 countries over a 32-year period. Nodes represent countries, and edge weights reflect the standardized total value of agricultural imports and exports between two countries.

³<https://zenodo.org/records/7213796#.Y1c06y8r30o>

- **UN Vote** is a DTGD documenting voting patterns in the United Nations General Assembly over more than 70 years. Nodes represent countries, and edge weights increase when two countries both vote “yes” on a motion.
- **Contact** tracks the physical proximity of approximately 700 students over a 1-month period. Nodes represent students, and edges denote proximity interactions, with weights indicating the duration or strength of physical closeness.

A.2 Descriptions of Baselines

The details of the nine baselines are described below:

- **JODIE** is tailored for temporal bipartite networks, such as user-item interactions. It utilizes two coupled recurrent neural networks to dynamically update the states of users and items upon interactions. A projection mechanism predicts future user/item embeddings by learning their temporal trajectory.
- **TGAT** utilizes graph attention mechanisms with temporal encoding to model node dynamics over time. This approach ensures effective representation learning by combining temporal and structural graph information .
- **TGN** uses a memory module for each node to maintain evolving states. These states are updated using message-passing paradigms, including a message function, aggregator, and updater. The embedding module further generates temporal node representations .
- **CAWN** adopts causal Anonymous Walks to capture causal patterns in dynamic graphs. Each walk is encoded with recurrent neural networks, and the results are aggregated for node representation. This method excels in leveraging temporal and causal graph structures .
- **EdgeBank** is a memory-based model dynamic link prediction. It retains observed edges in memory and predicts interactions based on past edge information. Variants like EdgeBank_{∞} and EdgeBank_{tw} adapt memory retention to different temporal contexts, such as fixed-size windows or edge appearance thresholds.
- **TCL** conses using a breadth-first search in temporal subgraphs. It applies a graph transformer that integrates graph topology and temporal attributes while modeling interdependencies via cross-attention mechanisms .
- **GraphMixer** introduces fixed time encoding and uses an MLP-Mixer architecture for link and node features to create effective representations. This model emphasizes simplicity while ensuring robustness across temporal graph tasks .
- **DyGFormer** integrates attention mechanisms for handling dynamic graph structures and temporal sequences. Its architecture features multiple transformer layers and employs co-occurrence and aligned encoding to enhance node representations. The model is highly adaptable, supporting varying sequence lengths and dynamic contexts.

A.3 Detailed Configurations

We present the hyperparameters and configurations of the model in Table 5. The datasets are split chronologically, with approximately 10% of the nodes designated as unobservable for the inductive learning task.

Table 5: GRN configurations and hyperparameters.

Configurations	Wikipedia	Reddit	MOOC	LastFM	Myket	Enron	Social Evo.	UCI	Flights	Can. Parl.	US Legis.	UN Trade	UN Vote	Contact
Train-Validate-Test Split	70%-15%-15%													
Node Embedding Size	64													
Time Embedding Dimension	64													
# Graph Retention Heads	2													
# Groups for GN	2													
Dropout	0.5	0.5	0.5	0.5	0.5	0.1	0.3	0.3	0.1	0.1	0.1	0.5	0.5	0.5
Weight Decay	0.001	0.001	0.001	0.001	0.001	0.0001	0.001	0.001	0.0001	0.0001	0.0001	0.001	0.001	0.001

B Detailed Experimental Performance

B.1 Evaluation Performance

Noe-level Classification Performance The datasets selected for the node classification task are Wikipedia with 5 classes of nodes and Reddit with 15 classes, both of which have nodes without raw features. It is worth noting that there is an imbalance in the distribution of node classes in both datasets.

Table 6: AP for inductive link prediction on dynamic graphs.

Datasets	JODIE	DyRep	TGAT	TGN	CAWN	TCL	GraphMixer	DyGFormer	GRN
Wikipedia	87.39±0.86	81.56±1.08	92.56±0.51	92.38±0.26	97.46±0.05	93.93±0.27	93.61±0.09	<u>98.32±0.05</u>	100.0±0.00
Reddit	94.71±0.29	91.08±1.03	92.54±0.28	90.50±1.60	98.16±0.03	88.66±0.12	92.46±0.04	<u>98.46±0.04</u>	99.99±0.02
MOOC	65.55±2.49	64.90±2.95	<u>74.72±2.24</u>	74.16±3.33	64.71±0.97	71.14±1.51	68.35±0.65	<u>64.39±0.94</u>	100.0±0.00
LastFM	82.39±0.63	80.54±0.90	75.17±0.20	65.89±6.42	87.55±0.09	71.85±0.20	81.63±0.20	<u>93.11±0.03</u>	99.79±0.47
Myket	<u>82.99±0.17</u>	80.50±0.55	60.99±4.85	61.30±5.02	77.76±0.24	63.27±2.72	80.50±0.03	<u>72.90±0.57</u>	100.0±0.00
Enron	70.92±2.88	59.47±1.42	66.30±0.67	68.25±1.70	82.58±0.57	67.73±2.17	74.44±0.48	<u>83.96±2.06</u>	97.53±4.70
Social Evo.	82.04±1.21	74.52±6.80	89.39±0.41	87.71±0.94	79.65±0.01	89.71±0.19	89.16±0.15	<u>92.50±0.11</u>	99.11±0.63
UCI	74.34±1.96	50.03±1.69	79.70±0.60	81.62±0.68	89.80±0.20	82.00±1.05	90.16±0.47	<u>93.78±0.07</u>	99.88±0.12
Flights	87.41±1.85	83.31±1.37	83.64±0.12	87.47±2.45	94.56±0.35	79.96±0.47	79.79±0.18	<u>97.43±0.05</u>	99.78±0.47
Can. Parl.	54.01±0.24	54.97±0.79	53.35±0.41	53.42±0.37	55.13±1.29	53.48±0.88	57.39±0.35	<u>81.86±0.69</u>	99.80±0.45
US Legis.	51.58±0.67	54.01±1.01	55.77±4.45	<u>59.69±0.15</u>	59.52±0.73	59.22±0.40	53.89±1.47	55.49±0.54	98.50±3.14
UN Trade	56.43±0.98	54.70±0.56	59.72±0.93	52.70±0.71	<u>63.29±0.16</u>	61.12±0.66	54.10±4.47	55.72±1.74	97.36±3.38
UN Vote	52.05±0.81	51.90±0.27	50.79±0.43	49.91±1.54	49.09±0.85	52.72±1.08	<u>54.43±0.43</u>	53.64±0.21	99.83±0.37
Contact	89.64±2.23	67.66±5.22	92.68±0.22	87.04±3.75	86.36±0.31	87.38±0.56	87.46±0.31	97.71±0.04	<u>96.30±3.90</u>
Avg. Rank	5.57	7.14	5.86	6.50	4.71	5.64	5.14	3.36	1.07

Table 7: AUC-ROC for inductive link prediction on dynamic graphs.

Datasets	JODIE	DyRep	TGAT	TGN	CAWN	TCL	GraphMixer	DyGFormer	GRN
Wikipedia	87.48±0.78	81.87±1.02	92.09±0.62	92.23±0.28	96.95±0.08	93.51±0.26	93.56±0.09	<u>98.11±0.07</u>	100.0±0.00
Reddit	94.52±0.24	91.47±1.02	92.90±0.18	91.40±1.19	97.78±0.04	89.11±0.12	92.39±0.03	<u>98.21±0.07</u>	99.99±0.01
MOOC	70.43±2.82	67.67±3.67	75.97±2.80	<u>76.07±3.82</u>	65.62±0.92	71.98±2.29	70.00±0.36	<u>65.56±1.02</u>	100.0±0.00
LastFM	81.85±0.84	79.72±0.90	74.67±0.18	64.02±5.23	85.07±0.14	69.83±0.18	80.35±0.05	<u>92.87±0.05</u>	99.79±0.48
Myket	<u>80.32±0.21</u>	78.56±0.52	60.37±5.60	59.88±6.34	74.54±0.22	60.91±2.46	77.67±0.06	<u>69.57±0.53</u>	100.0±0.00
Enron	74.03±2.46	59.83±1.33	64.13±0.96	67.50±1.46	82.16±0.55	65.46±2.49	75.70±0.60	<u>83.12±2.57</u>	97.34±5.12
Social Evo.	86.77±0.69	77.98±6.01	91.66±0.29	90.43±0.50	84.47±0.04	92.06±0.08	92.20±0.10	<u>94.90±0.07</u>	99.11±0.62
UCI	76.01±1.22	50.65±2.63	76.97±0.77	78.27±0.70	87.13±0.24	79.72±0.92	88.33±0.54	<u>91.54±0.11</u>	99.88±0.12
Flights	87.83±2.01	82.91±1.67	83.67±0.08	87.98±3.11	93.60±0.47	80.49±0.10	80.38±0.05	<u>97.35±0.09</u>	99.90±0.21
Can. Parl.	54.10±0.46	56.09±0.71	54.41±0.73	55.44±0.79	58.22±2.07	55.19±1.50	58.79±0.49	<u>84.95±1.06</u>	99.80±0.45
US Legis.	53.87±1.36	55.74±1.88	56.27±5.33	<u>60.25±0.34</u>	59.40±1.39	59.72±0.47	54.46±2.65	<u>53.46±0.65</u>	98.50±3.14
UN Trade	58.15±0.77	56.21±0.61	61.64±0.52	54.65±1.01	<u>65.05±0.18</u>	62.69±0.41	53.77±6.18	57.60±2.40	97.32±3.32
UN Vote	50.71±1.07	50.09±0.48	50.45±0.48	48.77±1.91	47.43±0.57	51.54±1.15	<u>53.55±0.38</u>	53.23±0.24	99.85±0.32
Contact	92.26±1.17	72.40±5.69	94.43±0.09	90.95±2.42	84.30±0.30	90.93±0.23	90.93±0.24	97.96±0.04	<u>95.95±4.41</u>
Avg. Rank	5.64	7.14	5.86	6.07	4.79	5.71	5.14	3.57	1.07

B.2 Training and Inference Performance

The training and inference performance of the baselines and our model are shown in Figure 4.

C Concerns and Limitations

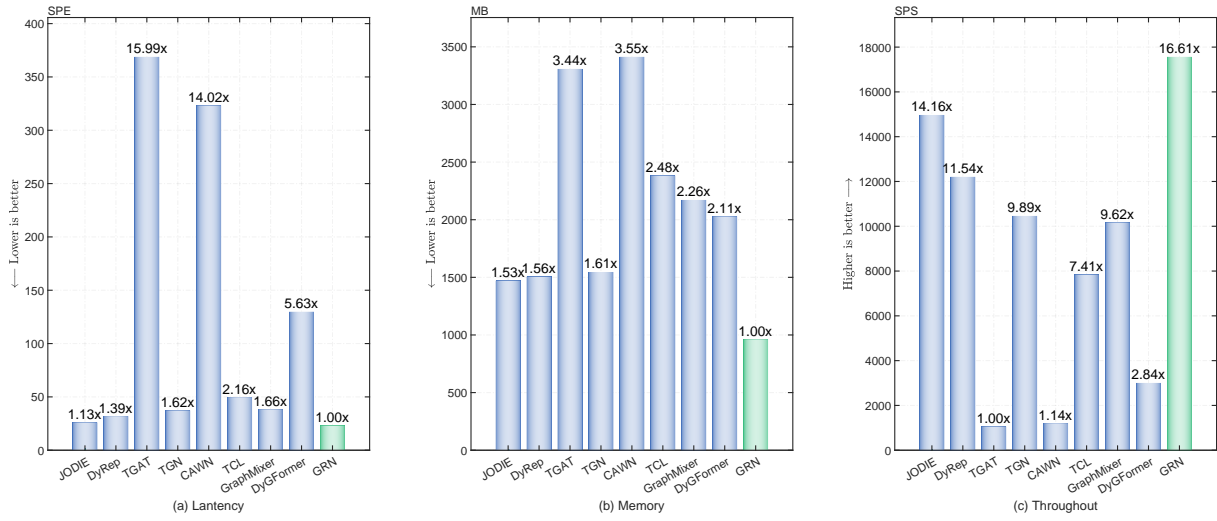
While the proposed GRN architecture demonstrates significant advancements, several limitations warrant further investigation. First, the near-perfect performance of GRN across multiple datasets raises concerns about potential over-fitting or dataset-specific optimizations. Despite thorough verification to ensure no leakage of information between training and test sets, such consistently high results may indicate the need for additional evaluations on more challenging and diverse benchmarks.

Second, the current design of GRN is limited to aggregating information from neighboring nodes, which restricts its ability to capture high-order dependencies. This limitation could hinder the model’s performance in scenarios requiring a deeper understanding of graph structure or relationships spanning multiple hops.

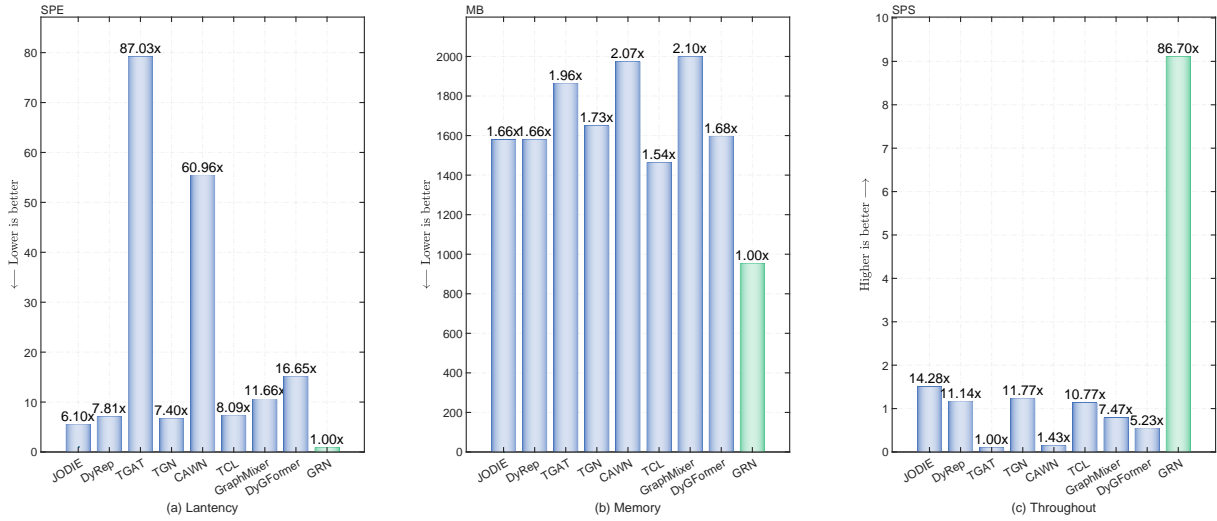
Lastly, while GRN retains substantial information through its recurrent state, the fixed dimensionality of this state presents scalability challenges. For super-large-scale and ultra-long-term dynamic graphs, increasing the dimensionality of the recurrent state may become necessary to avoid information bottlenecks. Such modifications, however, could introduce additional computational overhead, necessitating careful trade-offs between efficiency and expressiveness.

Table 8: AUC-ROC for node classification on dynamic graphs.

Datasets	JODIE	DyRep	TGAT	TGN	CAWN	TCL	GraphMixer	DyGFormer	GRN
Wikipedia	86.89±1.31	87.72±0.71	68.93±3.06	75.82±2.60	79.17±1.07	75.85±2.18	72.38±2.89	78.99±0.12	88.32±1.45
Reddit	64.82±1.77	<u>62.25±1.50</u>	61.07±1.32	57.11±1.46	59.84±0.07	61.44±1.11	60.53±0.59	61.85±0.57	61.10±0.72
Avg. Rank	2	1.5	7.5	8	6	5	7.5	4	3



(a) Training Performance.



(b) Inference Performance.

Figure 4: Training and inference performance comparison. Subfigure (a) compares the performance of the baseline with that of GRN when trained in the chunk-wise paradigm, and subfigure (B) compares the performance of GRN inference in the recurrent paradigm with that of the baselines. All multipliers are based on the model with the lowest value.